15 K EPR of an oxygen-hole boron centre, $[BO_4]^0$, in x-irradiated zircon

2000 J. Phys.: Condens. Matter 12 1441

(http://iopscience.iop.org/0953-8984/12/7/325)

J. Phys.: Condens. Matter **12** (2000) 1441–1450. Printed in the UK PII: S0953-8984(00)07504-4

15 K EPR of an oxygen-hole boron centre, $[BO_4]^0$, in x-irradiated zircon

C J Walsby, N S Lees, W C Tennant and R F C Claridge†

Department of Chemistry, University of Canterbury, Private Bag 4800, Christchurch, New Zealand

Received 3 September 1999

Abstract. Precise interaction matrices are reported for a boron-stabilized oxygenic-hole centre in x-irradiated zircon as derived from x-band electron paramagnetic resonance (EPR) measurements at ca 15 K. The presence of boron has been identified unequivocally through the observation and spin Hamiltonian analysis of superhyperfine structures from both naturally occurring isotopes of boron. Each of the parameter matrices indicates that the centre has point-group symmetry *m* (C_s), as is common in hole centres in zircon, where the hole centre is trapped on an oxygen atom within one of the crystal mirror planes. Analysis of the principal directions of these matrices indicates that the boron atom resides in a silicon position neighbouring the oxygenic electron vacancy.

1. Introduction

Zircon ($ZrSiO_4$) can be viewed as being constructed from covalently bonded SiO_4^{4-} tetrahedra constrained by electrovalent interactions with Zr^{4+} cations. As the only anion in the ideal zircon crystal lattice, O^{2-} serves as the only host for electron holes to be formed. With this in mind it is usual to consider the microstructure surrounding an oxygenic electron hole in zircon as based primarily on an SiO_4^{4-} tetrahedron. The space group of zircon is $I4_1/amd$ and the Zr and Si lattice positions have tetragonal point-group symmetry, $\bar{4}2m$ (D_{2d}). The ligand oxygen atoms lie within the crystal mirror planes and thus have point-group symmetry *m* (C_s). EPR studies of oxygenic hole centres in zircon produce spectra which, almost invariably, reflect Laue class $2/m$ for the site of the paramagnetic centre and point-group symmetry *m* can be inferred since O is the only ligand site available for trapping the electron hole.

EPR studies of oxygenic-hole centres in zircon created by ionizing radiation represent a surprisingly complex field. At least ten such centres have been confidently identified [1–3] with possibly twice this number reported [1] with structures not established unambiguously. This multiplicity of hole centres can be understood in terms of impurity atoms and defects within the crystal lattice. The centre discussed herein is representative of a particular class of these centres, which are created when an oxygenic hole is stabilized by a 3+ ion substituted at a neighbouring silicon position. Stability in these cases is achieved as the formation of the electron vacancy creates a site with an effective charge of +1 with respect to the local lattice. Substitution of a neighbouring Si^{4+} with a 3+ ion creates a negative charge which assists in the trapping of the oxygenic hole by creating a moiety with overall charge neutrality. Previously reported examples of this in zircon are $[AlO_4]^0$ [2] and $[AsO_4]^0$ [1]. In labelling such centres, the convention of Nuttall and Weil [4] for similar centres in α-quartz and Claridge *et al* [2]

† Author to whom all correspondence should be addressed.

0953-8984/00/071441+10$30.00

in studies of centres in zircon is followed and the overall charge of the centre assigned by comparison with the usual crystal lattice.

This report presents a detailed 15 K EPR study of a boron-containing oxygenic-hole centre observed first in a nominally undoped zircon crystal and subsequently in crystals deliberately doped with B_2O_3. Unequivocal identification of the impurity ion as boron has been achieved through observation of the superhyperfine structure due to both the ^{10}B and ^{11}B isotopes of boron and via fitting of the g_n matrix of the dominant (80.2% abundant) ^{11}B isotope. Precise interaction matrices $\bar{g}$, $\bar{A}(^{11}B)$, $\bar{P}(^{11}B)$ and $\bar{g}_n(^{11}B)$ are reported and used to determine the site of substitution, orbital occupancy and energy levels of this centre.

2. Experimental details

The crystal, the x-band Varian E12 spectrometer and the crystal goniometer used were as described earlier by Claridge *et al* [2]. The first spectra of the hitherto unreported centre were observed in a synthetic zircon crystal which was nominally undoped. It was grown by the Aerospace Corporation and cut to a parallelepiped (dimensions 5.5 mm × 3.5 mm × 2.0 mm) with faces parallel to the crystallographic a, b and c axes of the tetragonal system. Later, data were collected from crystals which were doped with B_2O_3 and grown using the flux growth technique, as described by Chase and Osmer [5]. The first observations of spectra from this centre were after the undoped crystal had been x-irradiated at room temperature using x-rays from a tungsten tube. In this case relatively narrow line widths (∼0.025 mT with $\boldsymbol{B} \parallel \boldsymbol{b}$ and ∼0.050 mT with $\boldsymbol{B} \parallel \boldsymbol{c}$) were observed, allowing full resolution of the often complex spectra. Similar results were obtained when the crystal was irradiated at 77 K and transferred cold to the previously chilled head of the Displex closed-cycle refrigeration system and then annealed to room temperature. Overlap with the thermally unstable $[AlO_4]^0$ [2] centre prevented measurement of the new centre directly after cold transfer. The centre was observed in the doped crystals following similar treatment, with irradiation at both RT and 77 K.

The first batch of doped synthetic zircons which produced well resolved spectra of the new centre was grown with 0.02% B_2O_3 and produced crystals with the typical zircon crystal growth habit being bi-pyramidally capped parallelepipeds. Inhomogeneity in the growth process was evidenced by varied colouration amongst the crystals from the same batch, with many being clear while others had yellow or brown tinting. After irradiation at 77 K the doped crystals took on a blue-black colouration which was removed when the crystal was heated to room temperature. These observations are usual in such experiments on zircons. However, when annealed to room temperature, the boron-doped crystals retained a strong purple-brown colouration. This faded slowly over a period of days but was still visible after several weeks. Such a room temperature stable colouration in zircon caused by irradiation appears to be quite rare. Similar effects were noted with *room temperature* irradiation of the boron-doped crystals with a distinct purple-brown tint again in evidence. The colouration was more intense in crystals from an earlier batch with 0.1% B_2O_3 doping. EPR experiments did not seem to indicate any correlation between the EPR signals and the colour.

All measurements were conducted at about 15 K. As the centre had the *m* symmetry typical of oxygenic-hole centres in zircon, sufficient data for the refinement of all matrix elements could be obtained by rotation in the *bc* plane only, using the technique of symmetry-related sites [6]. This was also convenient as the doped synthetic zircons used in these studies had natural faces which were parallel to the *ac* and *bc* crystal planes and thus allowed for very precise alignment of the crystals with respect to the static magnetic field. Data were collected at 10° increments in the *bc* plane through 90°.

3. Results

3.1. Spectra

As demonstrated by the experimental *c*-axis spectrum shown in figure 1(e), interpretation of this centre was initially complicated by the presence of many forbidden lines. As with the other hole centres exhibiting point-group symmetry m, the $[BO_4]^0$ centre showed a maximum site splitting of three in the *bc* plane, collapsing to two with $\boldsymbol{B} \parallel \boldsymbol{b}$ and one with $\boldsymbol{B} \parallel \boldsymbol{c}$. At some orientations, four equally spaced lines were observed which had intensities considerably greater than those from forbidden transitions and thus the centre was identified as involving an interaction with an isotopically dominant $I = 3/2$ nucleus.

3.2. Fitting

Examination of the results of the initial fitting of the g anisotropy confirmed that this was a previously unreported centre. As is common in hole centre analyses in zircon [2], it was clear that two off-diagonal g-matrix elements of the g matrix were zero within experimental uncertainty, confirming that the point-group symmetry of the site was m (C_s). Fitting of the hyperfine lines required the correct choice of the compensating nucleus and consequently the correct value of nuclear g. There are several elements with dominant isotopes having $I = 3/2$ which could potentially be found as impurities in zircon. Fortunately, all of these have relatively distinct g_n values which, in principle, should allow the correct nucleus to be identified. In the full analysis of the observed spectra the appropriate spin Hamiltonian is

$$\mathcal{H}_s = \beta_e \boldsymbol{S} \cdot \bar{g}_i \cdot \boldsymbol{B} + \boldsymbol{S} \cdot \bar{A}_i \cdot \boldsymbol{I} - \beta_n \boldsymbol{I} \cdot (\bar{g}_n)_i \cdot \boldsymbol{B} + \boldsymbol{I} \cdot \bar{P}_i \cdot \boldsymbol{I}. \tag{1}$$

In the above expression the subscript i refers to the $i = 1$–4 symmetry-related sites of the C_4 rotation group which is appropriate for sites of $2/m$ Laue class (point-group symmetries 2, m or $2/m$) in a tetragonal crystal. It is noted, however, that the full rotation group is D_4 [6]. Rather than fix the g_n matrix as the 3×3 unit matrix multiplied by an isotropic value for an assumed nucleus, it was constrained to be isotropic and fitted along with the elements of all the other parameter matrices using the programme EPR–NMR [7]. As shown in table 1, the final fitting was very precise with a root-mean-squared deviation (RMSD) of only 0.003 mT, being one-tenth of the average peak-to-peak linewidth of 0.03 mT. Consequently, as shown in table 1, the principal values and directions were also very well defined. Of particular interest was the g_n matrix which, within experimental uncertainty, had values in agreement to three significant figures with the isotropic atomic beam values [8] given for boron. Therefore, the compensating nucleus had been identified unambiguously from fitting of the experimental data alone. As a very precise fitting of the data had been achieved it was considered that anisotropy in g_n might be detectable. This was investigated by allowing the same elements as fitted in the other parameter matrices to be refined, but the result was a matrix which was isotropic within experimental uncertainty. The simulations of figure 1(a)–(d) demonstrate clearly, in comparison to the experimental spectrum in figure 1(e), the crucial role of g_n in analysing the EPR spectrum of the centre.

Although the fittings were convincing, the observation of lines due to the minor boron isotope are also important for an unequivocal assignment of this centre. Unfortunately, at almost all orientations in the *bc* plane, any lines due to ^{10}B (19.8% abundant, $I = 3$) were almost completely obscured by the many lines due to ^{11}B (80.21% abundant, $I = 3/2$). The exception to this was with the crystal *b*-axis aligned parallel to the static magnetic field, where the ^{11}B spectrum of the degenerate sites consisted almost exclusively of the four main allowed lines. As demonstrated in figure 2, this allowed for the measurement of all seven lines from the

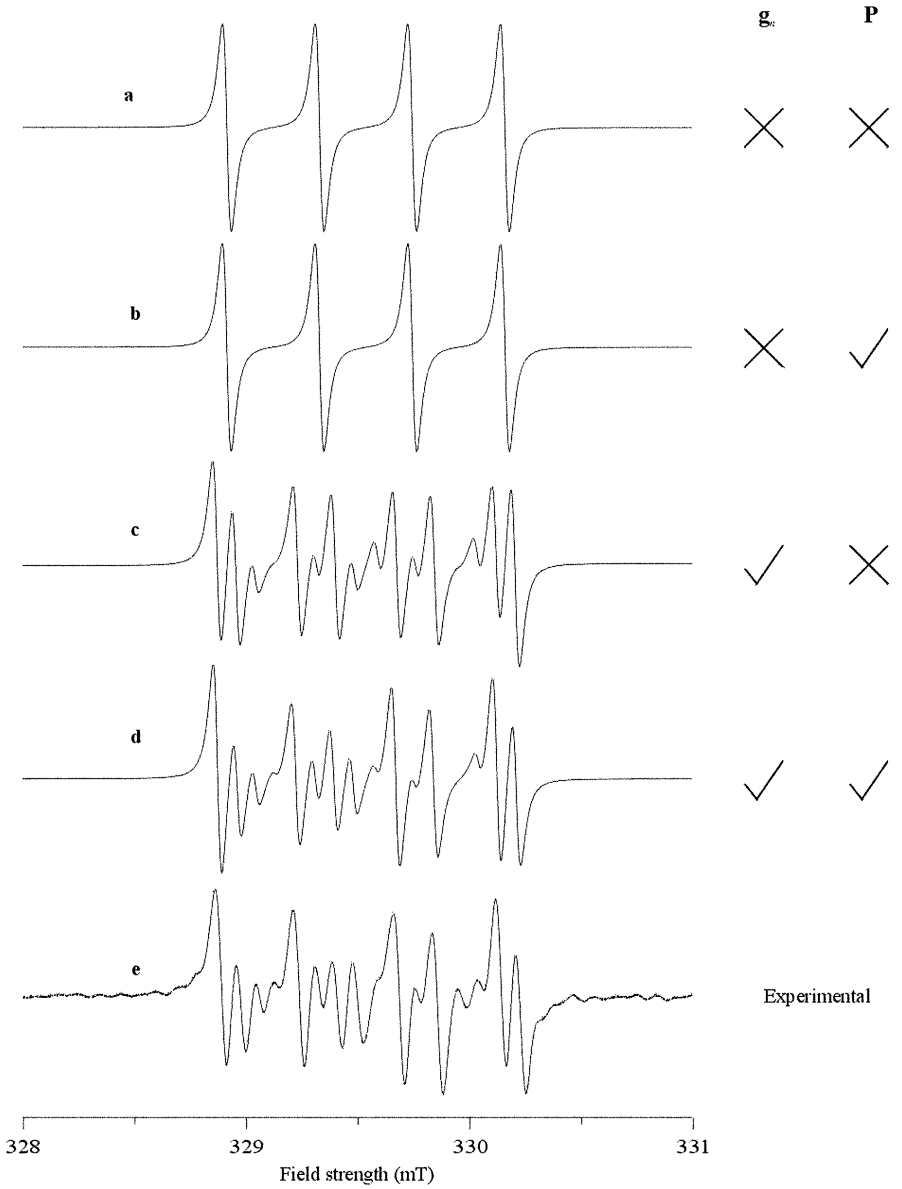

Figure 1. (a)–(d) calculated spectra showing the effects of $\bar{g}_n$ and $\bar{P}$ on the *c*-axis spectrum; (e) observed *c*-axis spectrum of the $[BO_4]^0$ centre.

less abundant $I = 3$ isotope and thus there could be no doubt that this centre contained boron. The measured hyperfine interaction constants for the two B isotopes should be proportional to their corresponding nuclear g values, i.e.,

$$\frac{g_n(^{10}\mathrm{B})}{g_n(^{11}\mathrm{B})} \approx \frac{A(^{10}\mathrm{B})}{A(^{11}\mathrm{B})}. \tag{2}$$

The ratio of the g_n values calculated using the literature values [9] is 0.334, while the ratio of the mean hyperfine splittings measured from the spectrum of the degenerate sites on the *b*-axis

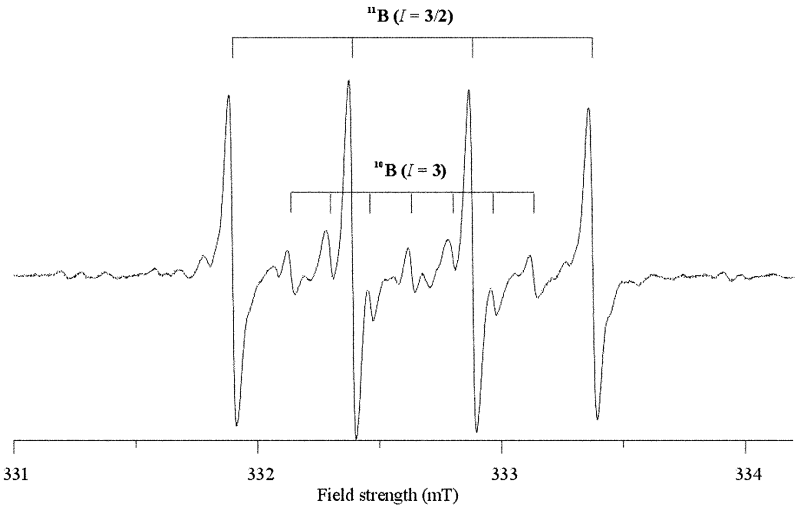

Figure 2. The b-axis spectrum of $[BO_4]^0$ showing hyperfine structures from both isotopes of boron; $\upsilon = 9.330$ GHz.

Table 1. Spin-Hamiltonian parameters for the $[BO_4]^0$ centre in zircon[a]. Number of unit-weighted data points = 94, sum of weighting factors = 138.4, RMSD = 0.003 mT.

		Matrix $\bar{Y}$		k	Principal value Y_k	Principal direction θ_k (deg)	Principal direction ϕ_k (deg)
$\bar{g}$	2.037702(2)	0	−0.015591(1)	1	2.047430(2)	58.04(0)	0
		2.003858(2)	0	2	2.012714(2)	148.04(0)	0
			2.022442(2)	3	2.003859(2)	90	90
$\bar{A}/g_e\beta_e$	−0.3201(4)	0	−0.1607(2)	1	−0.1904(3)	128.9(1)	180
(^{11}B) (mT)		−0.4884(3)	0	2	−0.4884(3)	90	90
			−0.3897(4)	3	−0.5193(2)	141.1(1)	0
$\bar{P}/g_e\beta_e$	0.0048(1)	0	−0.0057(1)	1	0.0082(2)	120.9(7)	0
(^{11}B) (mT)		−0.0035(2)	0	2	−0.0035(2)	90	90
			−0.0013(1)	3	−0.0047(2)	149.1(7)	180
$\bar{g}_n$	1.795(2)	0	0	1	1.795(2)	0	
		1.795(2)	0	2	1.795(2)	90	90
			1.795(2)	3	1.795(2)	90	0

[a] Error estimates in parentheses.

is 0.337. This excellent agreement confirms the earlier determination of the impurity ion as boron.

4. Discussion

It can be established via a crystal field analysis of the principal g values that oxygenic-hole centres in zircon formed by x-irradiation result from the trapping of an electron vacancy at a ligand oxygen atom. That is, an electron is removed and an unpaired electron is left in a p orbital of the ligand oxygen atom. The crystal field analysis makes it clear that the unpaired electron in the $[BO_4]^0$ centre is located in the non-bonding p_z orbital of the oxygen atom. Apart from the so-called C centre [10, 11] and one other [12], this appears to be the usual case for hole centres in zircon. The ground state configuration of the oxygenic hole is thus

$1s^2 2s^2 2p_x^2 2p_y^2 2p_z^1$. The lobes of the p_z orbital are directed perpendicular to the mirror plane containing the hole.

It is useful to compare the new $[BO_4]^0$ centre with the other well characterized similar centre $[AlO_4]^0$ [2]. Spin density calculations derived from the hyperfine matrices of each centre and the tables of Morton and Preston [13] have been determined. These indicate that only a small proportion of the spin density resides on the orbitals of the impurity atoms (5.04% on B in $[BO_4]^0$ and 2.08% on Al in $[AlO_4]^0$). In both calculations most of the spin density on the impurity atom is located in the p orbitals. Analysis of the g values establishes that it is the non-bonding p_z orbital which is the predominant site of the unpaired spin. As the formal configuration of B^{3+} is simply $1s^2$, it is proposed that this density may be found on the unoccupied 2p orbitals. A similar situation is expected to occur on Al^{3+} (configuration $1s^2 2s^2 2p^6$), with the density found on the unoccupied 3p orbitals rather than in the full 2p shell. One needs to add here a rider cautioning too much reliance on the Morton and Preston type analysis: B has no known cationic chemistry [14] and the bonding to O will be almost completely covalent with significant inclusion of B s, p orbital contributions to the resultant wavefunctions.

For sites of point-group symmetry *m* the only *requirement* of crystal symmetry is that one principal direction of each of the interaction matrices should lie along the inherent twofold axis, i.e., perpendicular to the mirror plane containing the site. However, as shown in table 2, there are marked correlations between the principal directions of the equivalent matrices in each centre to special directions in the unit cell of zircon (see figure 3). In both centres the largest and 'unique' g matrix principal direction lies close to the bond between the hole-bearing oxygen (fractional coordinates [0.32, 0, 0.07], O(1) of figure 3) and the neighbouring silicon atom, Si(1), at fractional coordinates [0.5, 0, 0.25]. (Fractional coordinates are with respect to Zr(0) of figure 3 as origin.) Both centres have another principal direction lying close to a Zr–O bond direction and the third constrained by symmetry to lie perpendicular to the mirror plane containing the atoms of interest. In the cases of the $A(^{11}B)$ matrix the largest 'unique' principal value lies just 2.6° away from the Si–O bond direction, while for the $A(^{27}Al)$ matrix the second to largest magnitude principal value lies 1.5° from this direction. The second principal directions are constrained to lie perpendicular to the mirror plane and the third appears to be directed close to an oxygen atom O(2) at fractional coordinates [0.68, 0, 0.07], although this may be coincidental. The principal directions of the P matrices are not dissimilar to those of the hyperfine matrices, but do not correlate as well with lattice atom positions or with each other. One expects the electric-field gradient at Si(1) to be dominated by the unpaired spin at O(1) and the Si–O direction to be a direction of the largest magnitude principal value to the quadrupole matrix, but this is obviously only approximately true. Overall, the orientations of the principal directions from all three parameter matrices are sensibly oriented in the unit cell, giving credence to the postulate that the impurity ion in each centre is located in the silicon atom position neighbouring the hole-bearing oxygen.

This assignment seems reasonable on the basis that aluminium and boron have far more in common with silicon in terms of chemistry than with zirconium. In addition, the ionic radius of Si^{4+} (0.42 Å) is far closer to that of B^{3+} (0.23 Å) and Al^{3+} (0.51 Å) than Zr^{4+} (0.79 Å), suggesting less distortion of the crystal lattice is required in the formation of each centre. On the basis of similar reports of aluminium centres in α-quartz [4], it is well known that aluminium will substitute into SiO_4^{4-} tetrahedra. We are not aware of any other paramagnetic B-stabilized hole centre.

The unusually complicated spectra of the $[BO_4]^0$ centre can be ascribed almost completely to the effect of the nuclear Zeeman interaction on the hyperfine energy levels (figure 1). Although the effect of $\bar{P}(^{11}B)$ on the overall appearance of the spectrum is relatively subtle,

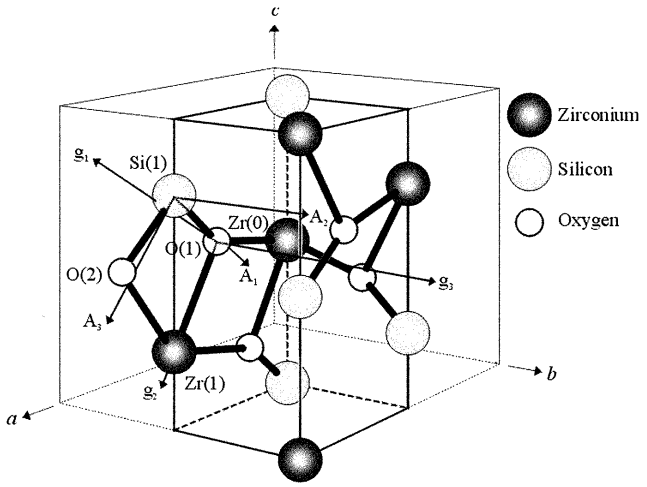

Figure 3. Portion of the unit cell of zircon depicting the orientations of the g and $A(^{11}\mathrm{B})$ principal directions for the $[BO_4]^0$ centre.

Table 2. Comparison of parameter-matrix principal directions and crystallographic atom positions for the $[BO_4]^0$ and $[AlO_4]^0$ (data from [2]) centres. Fractional coordinates of atoms are referred to Zr(0) of figure 3 as origin.

$[BO_4]^0$			$[AlO_4]^0$				Data		
k	θ_k	ϕ_k	k	θ_k	ϕ_k	Crystallographic direction to:	θ	ϕ	r (Å)
g matrices						Hole centre at O(1) (0.32, 0, 0.07)			
1	58.04	0	1	62.78	0	Si(1) (0.5, 0, 0.25)	48.5	0	1.623
2	148.04	0	2	152.75	0	Zr(1) (0.5, 0, −0.25)	147.6	0	2.267
3	90	90	3	90	90	⊥ to mirror plane			
A matrices						Impurity atom at Si(1) (0.5, 0, 0.25)			
1	128.9	180	2	133.0	180	O(1) (0.32, 0, 0.07)	131.5	180	1.623
2	90	90	3	90	90	⊥ to mirror plane			
3	141.1	0	1	137.0	0	O(2) (0.68, 0, 0.07)	131.5	0	1.623
P matrices						Impurity atom at Si(1) (0.5, 0, 0.25)			
1	120.9	180	1	158.4	180	O(1) (0.32, 0, 0.07)	131.5	180	1.623
2	90	90	2	90	90	⊥ to mirror plane			
3	149.1	0	3	111.6	0	O(2) (0.68, 0, 0.07)	131.5	0	1.623

the sign of its elements is still critical to correct fitting of the data. Simulation of the spectrum using the matrices from the data fitting but with various sign combinations of $\bar{A}(^{11}\mathrm{B})$ and $\bar{P}(^{11}\mathrm{B})$ confirmed that their relative signs are fixed. This is as expected for matrices which describe interactions with the same spin. The absolute signs of these matrices cannot be determined with respect to the g and $g_n(^{11}\mathrm{B})$ matrices from the EPR data. In the report of the $[AlO_4]^0$ centre in zircon [2] the hyperfine matrix was assigned a negative value and $\bar{P}$ a positive value, by following the reasoning of Nuttall and Weil [4] on the corresponding centre in α-quartz. The isotropic part of the hyperfine matrix, a, corresponding to the Fermi contact interaction is clearly dominant in both centres. For positive g_n ($g_n(^{27}\mathrm{Al}) = +1.4556601$), $a(^{27}\mathrm{Al})$ takes a negative value. Therefore, the sign of all three principal values of $\bar{A}(^{27}\mathrm{Al})$ must also be negative. As the signs of the elements of $\bar{P}$ are known with respect to those of $\bar{A}$, the sign of the electric field gradient for $[AlO_4]^0$ in both zircon and quartz at $^{27}\mathrm{Al}$ is

found to be positive. ^{11}B has a g_n value similar to that of ^{27}Al($g_n(^{11}\mathrm{B}) = +1.792424$) and it is assumed therefore that the isotropic part of the hyperfine interaction will have the same sign as for the $[AlO_4]^0$ centres in quartz and zircon. However, in the case of $[BO_4]^0$ the hyperfine matrix is considerably more anisotropic so it is not possible to be so confident in the assignment of the overall sign. Nevertheless, as shown in table 1, this has been given an overall negative sign and the quadrupole matrix assigned a positive value, as determined from A. The observation that the quadrupole matrices in both zircon centres have the same sign arises because the corresponding electric quadrupole moments also have the same sign ($Q(^{27}\mathrm{Al}) = 0.150$ compared with $Q(^{11}\mathrm{B}) = 0.040$) $\times$ |e| $\times 10^{-24}$ cm^2.

The g values of both $[BO_4]^0$ and $[AlO_4]^0$ have been analysed to determine the p-orbital splittings. The 6×6 complex matrix of the crystal-field spin–orbit coupling Hamiltonian block diagonalizes into two 3×3 matrices, numerical diagonalization of which produces three Kramers' doublets and their corresponding eigenvectors. The g values of the ground state can be calculated from these eigenvectors and the magnetic field Hamiltonian:

$$\mathcal{H}_{Zeeman} = \beta_e(\boldsymbol{l} + \alpha g_e \boldsymbol{s}) \cdot \boldsymbol{B} \tag{3}$$

where $\alpha > 1$ allows the p_z ground-state g_z value to exceed the free electron value. α is an empirical factor and can be regarded as a measure of the delocalization of the unpaired electron on the hole-bearing oxygen ion to other ions in the local lattice causing the centre to become more 'hole-like' in character. This may include s–p hybridization and exchange interactions through overlap with B s, p orbitals. For both hole centres the experimental g values were least-squares fitted to those calculated by iteratively stepping the orbital splittings. Since orbital reduction factors were not known and not obtainable from the EPR experiments it was found convenient to obtain the orbital splittings as dimensionless quantities Δ/ζ where Δ is the splitting and ζ the spin–orbit coupling constant. In each case the g values were fitted to within experimental uncertainty. The ordering of the p-orbital energy levels was found to be the same in both centres with similar splittings, and with p_y lying nearest to the ground state p_z level and p_x somewhat higher. These results are summarized below.

Dimensionless orbital splitting	$[BO_4]^0$	$[AlO_4]^0$
$(E_{p_x} - E_{p_z})/\zeta$	221.5	192.6
$(E_{p_y} - E_{p_z})/\zeta$	46.18	42.88

The ground state wavefunctions are for $[BO_4]^0$:

$$|\Psi_\pm\rangle = 0.99994|p_z\rangle \mp 0.00223|p_x\rangle - i0.01080|p_y\rangle;\ \alpha = 1.00096 \tag{4}$$

and for $[AlO_4]^0$:

$$|\Psi_\pm\rangle = 0.99993|p_z\rangle \mp 0.00257|p_x\rangle - i0.01163|p_y\rangle;\ \alpha = 1.00147. \tag{5}$$

It is conceded that the accuracy of these calculations is limited through neglect of covalency and s-orbital mixing with the excited state $1s^2 2s^1 2p^6$ configuration. Nevertheless, they adequately describe the ordering of the p-orbital energy levels and give a good measure of their separations. Taking [15, 16] $\zeta = -135$ cm^{-1} the splittings for the $[BO_4]^0$ centre are 29 903 and 6234 cm^{-1}.

It is of interest to compare the hyperfine and quadrupole matrices for the two above centres. For similar geometries and bondings one might have expected that the ratios of the isotropic and anisotropic constants, a and b, respectively derived from the hyperfine matrices of the $[AlO_4]^0$ and $[BO_4]^0$ centres, would be given to a first approximation by the ratios of the Morton and Preston constants A and p [13] derived from Herman and Skillman wavefunctions [17].

We find experimentally for the isotropic parts, $a_{Al}/a_B = 1.91$ compared to the Morton and Preston prediction 1.54, i.e., rather poor agreement. For the anisotropic parts the picture is much worse. Experimentally we find $b_{Al}/b_B = 0.44$, whereas the predicted ratio is 1.31. Clearly the bonding in the two cases must be quite different and one would need to include overlaps between B and O orbitals for an adequate description.

Crudely one might expect the electric quadrupole interaction to be dominated by the electric-field gradient from the electron hole, on O. A simple point-dipole calculation of the electric-field gradient (efg) at B was carried out and the contribution to P_3 ($\sim 2P_\parallel/3$) calculated from the equation

$$P_\parallel = 3e^2qQ/4I(2I-1) \tag{6}$$

where $eq(=V_{zz})$ is the z component of the electric-field gradient and Q is the nuclear electric quadrupole moment. This led to $P_3 = 0.005$ mT with $\theta = 124.8^\circ$ and $\phi = 180^\circ$, in reasonable agreement with the experimental values of table 1. The agreement is probably fortuitous, however, in view of the neglect of all other lattice contributions to the efg but, more particularly, neglect of covalency which as discussed above is almost certainly important.

A measure of the distortion to the local crystal lattice created by the presence of the Al and B impurity ions can be determined by consideration of the so-called asymmetry parameter, η, which is a measure of the deviation of the electric-field gradient about the quadrupolar nucleus from uniaxial symmetry. This is defined by $\eta = (P_1 - P_2)/P_3$ (where P_3 is the 'unique' principal value). $\eta = 0$ for completely uniaxial symmetry and 1 for the maximum distortion from this symmetry. In the case of the $[AlO_4]^0$ centre, the Al(Si) site is distorted considerably from uniaxial symmetry, as evidenced by a value of $\eta = 0.703$. However, in the case of $[BO_4]^0$, the distortion at the B(Si) site appears quite small, with $\eta = 0.146$. This may be a consequence of the very different sizes of the respective ions: the radius of Al^{3+} is 0.51 Å, somewhat larger than Si^{4+} (0.42 Å), while the 'ionic' radius of B^{3+} is only 0.23 Å. As already emphasized, the bonding to B is expected to be almost completely covalent. One expects also [14] that there will be considerable bond shortening and the BO_4 unit will be rather smaller than SiO_4 in the ideal zircon lattice and considerably smaller than the corresponding AlO_4 unit. The quadrupole matrix for $[AlO_4]^0$ reflects strong influence from nearest-neighbour in-plane Si, Zr and hole-containing O atoms: the symmetry of the matrix is m as expected, but there is no well defined 'unique' principal direction—the largest principal direction lies almost mid-way between Zr and the hole-containing O (refer to figure 3). For $[BO_4]^0$, on the other hand, the quadrupole matrix is dominated by the efg arising from the hole on O(1) (figure 3) and the distortion from uniaxial symmetry is smaller by a factor of about five.

Acknowledgments

The authors thank the University of Canterbury Research Committee and the New Zealand Lotteries Board for grants towards equipment purchase and they acknowledge useful discussions with Professor J-M Spaeth of Universität Paderborn.

References

[1] Krasnobaev A A, Votyakov S L and Krochalev V Ya 1988 *Spektroskopya Tsirconov, Svoistva, Geologicheskie Prilozheniya* (Mosocw: Nauka)
[2] Claridge R F C, Mackle K M, Sutton G L A and Tennant W C 1994 *J. Phys.: Condens. Matter* **6** 10 415–22
[3] Barker P R and Hutton D R 1973 *Phys. Status Solidi* b **60** K109–11
[4] Nuttall R H D and Weil J A 1981 *Can. J. Phys.* **59** 1696–708
[5] Chase A B and Osmer J A 1966 *J. Electrochem. Soc.* **113** 198–9
[6] Weil J A, Buch T and Clapp J E 1973 *Adv. Magn. Reson.* **6** 183–257

[7] Mombourquette M J, Weil J A and McGavin D G 1996 *Computer Program EPR–NMR* (Canada: University of Saskatchewan)
[8] Raghaven P 1989 *At. Data Nucl. Data Tables* **42** 189–291
[9] Weil J A, Bolton J R and Wertz J E 1994 *Electron Paramagnetic Resonance: Elementary Theory and Practical Applications* (New York: Wiley)
[10] Claridge R F C, Sutton G L A and Tennant W C 1998 *J. Magn. Reson.* **125** 107–13
[11] Claridge R F C, Tennant W C, Schweizer S and Spaeth J-M 1999 *J. Phys.: Condens. Matter* **11** 8579–89
[12] Claridge R F C, Lees N S, Tennant W C and Walsby C J 2000 *J. Phys.: Condens. Matter* **12** 1431–40
[13] Morton J R and Preston K F 1973 *J. Magn. Reson.* **30** 577–82
[14] Cotton F A and Wilkinson G 1988 *Advanced Inorganic Chemistry, A Comprehensive Text* 4th edn (New York: Wiley)
[15] Bartram R H, Swenberg C E and Fournier J T 1965 *Phys. Rev.* A **139** 941–51
[16] Stapelbroek M, Bartram R H, Gilliam O R and Madacsi D P 1976 *Phys. Rev.* B **13** 1960–6
[17] Herman F and Skillman S 1963 *Atomic Structure Calculations* (Englewood Cliffs, NJ: Prentice-Hall)